Relaxation and dynamics of the (111) surfaces of the fluorides CaF_2 and SrF_2

1993 J. Phys.: Condens. Matter 5 5401

(http://iopscience.iop.org/0953-8984/5/31/005)

J. Phys.: Condens. Matter 5 (1993) 5401–5410. Printed in the UK

Relaxation and dynamics of the (111) surfaces of the fluorides CaF_2 and SrF_2

A Jockisch†, U Schröder†, F W de Wette‡ and W Kress§
†Universität Regensburg, D–93040 Regensburg, Federal Republic of Germany
‡Department of Physics, University of Texas, Austin, TX 78712-1081, USA
§Max-Planck-Institut für Festkörperforschung, D–70506 Stuttgart 80, Federal Republic of Germany

Received 28 May 1993

Abstract. We have treated the relaxation and the dynamics of the (111) surfaces of the fluorides CaF_2 and SrF_2 in the framework of shell models, in which the short-range interactions are represented by Born–Mayer potentials. The relaxation in the outer layer of the crystal, consisting of three closely spaced F–Ca/Sr–F layers, is significant.

The calculated normal vibrations of a 19-layer slab are presented in 3-dimensional diagrams of the normalized surface squared amplitude, which provide a very direct and pictorial display of the surface localization of vibrational states. For CaF_2 the calculations are compared with the HREELS data of Longueville *et al*.

1. Introduction

Calcium fluoride (CaF_2), which appears in nature as the mineral fluorite, is of technological interest because of its favourable properties as an ionic conductor. Moreover, CaF_2 and other fluorides such as SrF_2 are attractive materials for surface studies: experimentally because they are easily cleaved along (111) planes and the surface preparation is simple, and theoretically because of their predominantly ionic character; this allows the use of shell models to describe the ionic interactions.

In this paper we evaluate the relaxation and the dynamics of 19-layer (111) slabs of CaF_2 and SrF_2. This study is of interest firstly because of recent high-resolution electron energy loss spectroscopy (HREELS) measurements of the surface dynamics of CaF_2(111) by Longueville *et al* [1], and secondly because the present approach goes significantly beyond earlier treatments of the CaF_2(110) surface [2,3], which did not take into account surface relaxation and were carried out with the rigid ion model.

Our calculations are based on shell models which are reported in the literature [4,5]. The use of *bulk* shell models for these surface calculations is justified by the fact that these fluorides have closed shell electronic configurations which are only minimally disturbed by the presence of a surface and by changes in interionic distances resulting from relaxation.

The formalism used in the relaxation and the dynamical calculations is briefly outlined in section 2. The results of the relaxation calculations are presented in section 3, and those of the dynamical calculations in section 4.

2. Formalism (cf [6])

Shell models take into account long-range Coulomb interactions, short-range overlap

0953-8984/93/315401+10$07.50

interactions, and the most important aspects of the displacement-induced deformations of the electronic charge distributions in the dipole approximation. The calculations were carried out for slab-shaped fluorite-structure crystals bound by two parallel (111) faces. As customary in most shell model calculations, the short-range interactions were considered (a) between the core and the shell on the same ion by force constants k_i, (leading together with the shell charge Y_i to the ionic polarizability α_i), and (b) between the shells of neighbouring ions by longitudinal and transverse force constants, A_i and B_i, respectively.

Since a relaxation calculation requires a continuous variation of the interparticle distances, the interactions need to be expressed in terms of potentials. In addition to the Coulomb potentials for the long-range interactions, we represent the short-range interactions by Born–Mayer potentials

$$V_{ij}^{SR}(r) = a_{ij} \exp(-b_{ij} r) \,. \tag{1}$$

Lehner *et al* [7] have already tested the validity of these potentials and have shown that ionic pair potentials of this kind, which were derived for alkali halides and crystals with fluorite structures, could be carried over to perovskite structures, in which the interparticle distances of the ion pairs are different. This result also implies that near or at the surface no significant changes occur in the form of these potentials, so that they can be expected to lead to reliable results for surface relaxation. This has also been assumed to be the case in relaxation calculations for the alkali halides [8], the fluoridic perovskites $KZnF_3$ and $KMnF_3$ [6(a)], and $SrTiO_3$ [9]. The agreement of the calculated relaxation pattern for the SrO(100) surface of $SrTiO_3$ with the results of recent LEED measurements supports these assumptions.

The longitudinal and transverse force constants A_{ij} and B_{ij} of an ion pair (i, j), which enter into the dynamical matrix are given by

$$A_{ij}\left(\frac{e^2}{2v}\right) = \frac{\partial^2}{\partial r^2} V_{ij}^{SR}(r)\bigg|_{r=r_{ij}^0} \qquad B_{ij}\left(\frac{e^2}{2v}\right) = \frac{1}{r}\frac{\partial}{\partial r} V_{ij}^{SR}(r)\bigg|_{r=r_{ij}^0} \tag{2}$$

where e is the electronic charge, v the volume of the unit cell, and r_{ij}^0 the equilibrium distance of the ions i and j. Inversely, the potential parameters a_{ij} and b_{ij} of a given interaction can be obtained from the short-range force constants A_{ij}^0 and B_{ij}^0 that have been determined for a given bulk shell model by an appropriate fit to experimental phonon dispersion data. It is important to keep in mind that a relaxation procedure can only lead to converging results if the interaction potentials satisfy the static equilibrium condition of the crystal. A violation of the Cauchy relation $C_{12} = C_{44}$ is an indication of the presence of non-central components in the short-range forces. These non-central components are usually implicitly contained in the transverse force constants B as they are obtained from the fit to the experimental phonon dispersion curves; we may thus write,

$$B = B_c + B_{nc} \tag{3}$$

where B_c and B_{nc} are the central and the non-central parts of the transverse force constant, respectively. However, the static equilibrium condition of the crystal contains only the central parts B_c (cf [6(a)]). For the fluorite structure crystals the equilibrium condition has the form (written here for CaF_2):

$$\alpha_M Z^2 + B_c^{Ca-F} + B_c^{F_1-F_2} + 4B_c^{F_1-F_1} + 2B_c^{Ca-Ca} = 0. \tag{4}$$

Here α_M is the Madelung constant of the fluorite structure ($\alpha_M = 5.0388$), Z is the ionic charge of the cation and the B_c^{A-B} are the transverse force constants of the repulsive central interaction between ions A and B.

The calculations have been performed with shell models for CaF_2 and SrF_2 which are available in the literature [4, 5], except for minor adjustments in the transverse force constants B^{Ca-F} and B^{Sr-F}, respectively, to assure that equation (4) is satisfied in both cases. The model parameters are given in table 1.

Table 1. Parameters of the shell models for CaF_2 and SrF_2.

	Short-range force constants ($e^2/2v$)							
	Ca(Sr)–F		F^1–F^2†‡		Ca(Sr)–Ca(Sr)		F^1–F^1	
Compound	A_1	B_1 (B_{nc})	A_2	B_2	A_3	B_3	A_4	B_4
CaF_2	29.2	−3.12 (−0.074)	2.78	0.12	0.70	−0.52	−0.32	0.116
SrF_2	33.8	−4.06 (−0.0212)	0.86	0.16	0	0	0	0

	Ionic charge (e)	Shell charges (e)		Shell–core force constants (e^2/v)	
	F	Ca(Sr)	F	Ca(Sr)	F
Compound	Z	Y_1	Y_2	k_1	k_2
CaF_2	−0.970	5.183	−3.224	659.278	971.672
SrF_2	−1.6	7.202	−2.778	1298.251	643.691

† F^1 and F^2 are the fluorine ions above and below the Ca(Sr) planes, respectively.

‡ In these shell models, which were obtained from best fits to the measured phonon dispersion curves, A_2 and B_2 have the same sign, which is inconsistent with a Born–Mayer interaction between F^1 and F^2. This inconsistency can be removed by including a van der Waals interaction between F^1 and F^2. However, since this interaction is quite weak, and since the relaxation results in only a minimal change in the F^1–F^2 (second neighbour) distance, we have used these force constants as given in the literature [5, 6].

3. Relaxation

Surface relaxation and reconstruction are the result of the imbalance of the forces acting on the ion cores and shells, when the ions at or near the surface are in their unrelaxed bulk positions. Because of its high symmetry (cf figure 1) the (111) surface of the fluorite structure will only exhibit *relaxation*, i.e. displacements occur only in the direction normal to the surface. The relaxation was calculated by the same procedure as was applied to the alkali halide (001) surfaces [8], and to the fluoridic perovskites [6(a)]. For details and comments about the method used we refer the reader to these earlier publications.

The calculations were performed for 19-layer (111) slabs of CaF_2 and SrF_2, in which seven layers on each side of the slab were allowed to relax. The relaxation results are presented in table 2. To judge the size of these relaxations we note that at the *unrelaxed* surface (cf figure 1(*b*)) the two outer planes of fluorine ions are lying a distance $d = a/(4\sqrt{3})$ ($= 0.144\,a$; a is the lattice constant) above and below the first plane of alkali earth ions, respectively. It follows from table 2 that at the relaxed surfaces the distance between the top plane of fluorine ions and the next plane of alkali earth ions is diminished in CaF_2 by about 19% and in SrF_2 by about 9% of the lattice constant a, which corresponds to 28% and 14% of the interplanar distance d, respectively. In the deeper layers the relaxation decreases rapidly, similar to what was found for the alkali halides [8] and fluoridic perovskites [6(a)].

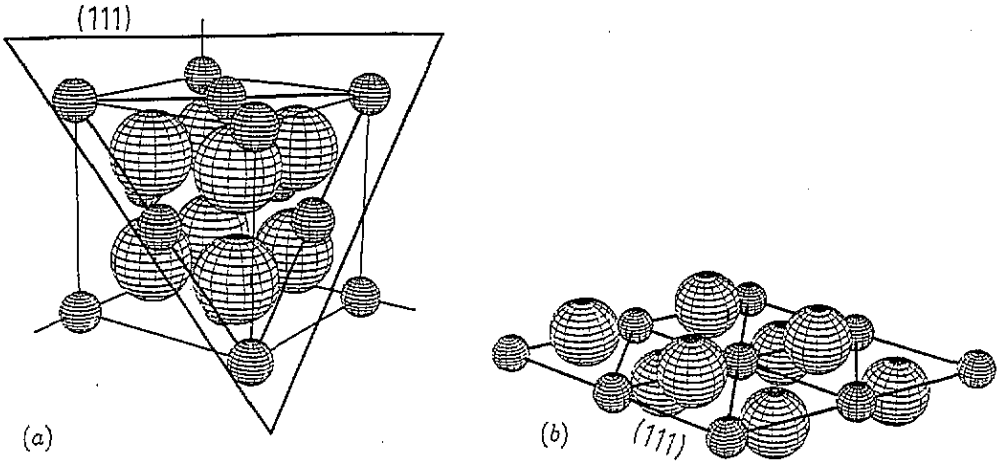

Figure 1. (*a*) Cubic unit cell of CaF_2 and SrF_2 with (111) cleavage plane indicated. (*b*) (111) surface plane of CaF_2 and SrF_2.

Table 2. Relaxation of the three outer layers of the $CaF_2(111)$ and $SrF_2(111)$ slabs, in units of the lattice constant (seven layers were allowed to relax).

Layer		F^1	Ca	F^2
1	core	−0.0246	0.0034	−0.0052
1	shell	−0.0260	0.0002	−0.0052
2	core	0.0028	0.0000	0.0002
2	shell	0.0029	0.0002	0.0002
3	core	−0.0001	0.0000	0.0000
3	shell	−0.0001	0.0000	0.0000
		F^1	Sr	F^2
1	core	−0.0129	0.0008	−0.0030
1	shell	−0.0154	−0.0012	−0.0031
2	core	0.0017	0.0000	0.0001
2	shell	0.0018	0.0002	0.0001
3	core	0.0000	0.0000	0.0000
3	shell	0.0000	0.0000	0.0000

4. Dynamics of the relaxed slab

The force constants for the relaxed slab were determined from the second derivatives of the pair potentials (Coulomb and Born–Mayer); the other parameters (Z_i, Y_i, k_i) were kept at their bulk values. With these coupling constants, the dynamical matrix was constructed and the vibrational spectra were obtained by diagonalization of the dynamical matrix for two-dimensional wave vectors $\bar{q}$ along the high-symmetry directions $\overline{\Gamma}\,\overline{K}$, $\overline{\Gamma}\,\overline{M}$ and $\overline{K}\,\overline{M}$ of the surface Brillouin zone (SBZ) (cf figure 2). Due to symmetry, there are six $\overline{\Gamma}\,\overline{M}$ directions, three of these point in the direction of fluorine ions *above* the alkali earth plane, and three to those *below* this plane. Accordingly, there is a small difference in the lowest bulk band edge at $\overline{M}$, between the two sets of directions, which, however, is too small to be of interest.

The slab dispersion curves for the 19-layer CaF_2 (111) slab are plotted in figure 3,

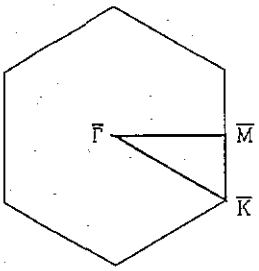

Figure 2. Two-dimensional surface Brillouin zone (SBZ) for the (111) surface of CaF_2 and SrF_2. An irreducible element $\bar{\Gamma}\ \bar{M}\ \bar{K}$ is delineated by a bold outline.

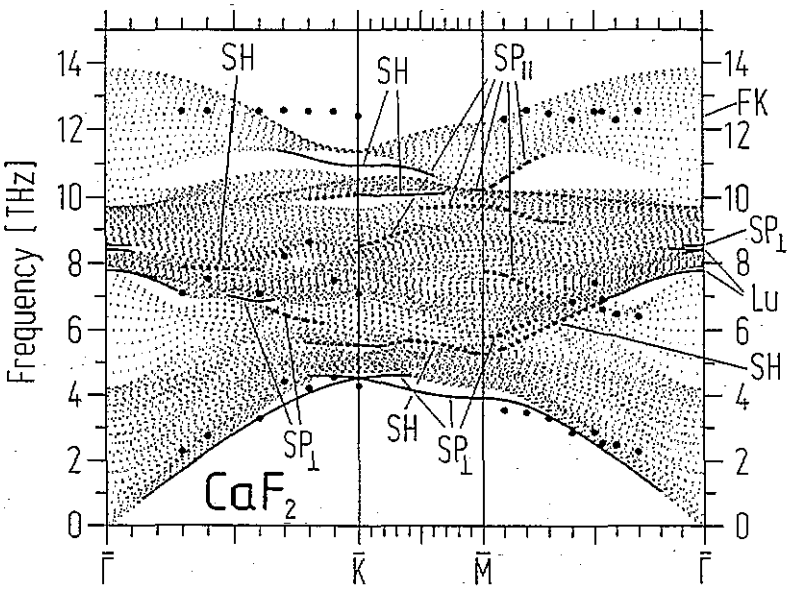

Figure 3. Dispersion curves for a 19-layer slab of CaF_2 with free (111) surfaces. The dotted lines are the bulk dispersion curves. The full and dashed lines are surface-localized modes and resonances, respectively. The experimental points are from [1].

together with the HREELS measurements of Longueville *et al* [1]. The dotted lines represent the bulk modes of the slab. Since the bulk unit cell contains three particles (nine degrees of freedom), there are nine bulk dispersion curves, three of which are acoustic and six optic. In the slab this gives rise to a total of nine *bulk bands*, again three acoustic and six optic. Each of these bands can give rise to surface localized modes or resonances (in figure 3 these are indicated by bold and dashed bold lines, respectively). Which kind of surface modes and resonances occur for each individual compound is determined by the structure of gaps between the bulk bands and by the way the bands overlap. Because the mass ratio of Ca and F is not large (≈ 2), there is significant overlap of the bulk bands, with the result that there are relatively few well-pronounced surface modes and relatively many surface resonances. In figure 3 the surface modes and resonances have been labeled according to their predominant vibrational character: SP stands for sagittal plane (plane through the surface normal and the wave vector); $SP_\perp$ and $SP_\parallel$ are vibrations in the SP, predominantly perpendicular and parallel to the surface; SH (shear horizontal) indicates

vibrations perpendicular to the SP. For a more detailed discussion of the character and the classification of these surface modes we refer the reader to Kress *et al* [10] as well as to [6(a)].

The identification of surface modes and surface resonances is in principle done by examination of the vibrational amplitudes of the modes as functions of the distance from the surface. However, a convenient way to obtain the most important information in this respect is to display, in a three-dimensional plot, the participation of the surface particles in the slab modes contained in two-dimensional (2D) intervals $\Delta\bar{q}\Delta\omega$ of the dispersion curve diagram (figures 3 and 6). Let $\xi_\alpha(l\kappa;\bar{q}\,p)$ be the α-component of the polarization vector, associated with particle κ in layer l in the mode characterized by the 2D wave vector $\bar{q}$ and polarization index p (= $1,\ldots,3n$; n is the number of particles in the slab unit cell). Since we want to display the predominant vibrational character of the surface modes we choose a representation in which α represents the mutually orthogonal $SP_\perp$, $SP_\parallel$ and SH directions. Then the appropriate quantity to be plotted is the *normalized surface squared amplitude*:

$$A_\alpha(l=1;\bar{q}\,\omega)=\frac{1}{g(\bar{q},\omega)}\sum_{\substack{\kappa\\(l=1)}}\sum_{p}|\xi_\alpha(l=1,\kappa;\bar{q}\,p)|^2\,\delta(\omega-\omega_p(\bar{q})). \quad (5)$$

Here, $l=1$ singles out the surface layer and $g(\bar{q},\omega)$ is the density of slab modes in $(\bar{q},\omega)$-space, (i.e. $g(\bar{q},\omega)\Delta\bar{q}\Delta\omega$ is the number of slab modes whose $\bar{q},\omega$-values lie in $\Delta\bar{q}\Delta\omega$). The division by $g(\bar{q},\omega)$ assures that the accumulation of a large number of bulk contributions in a given 2D interval $\Delta\bar{q}\Delta\omega$, does not result in the appearance of a spurious surface mode or resonance in that interval. The function A_α is displayed for CaF_2 and SrF_2 in figures 4 and 7, respectively, in separate panels representing successively the $SP_\perp$, $SP_\parallel$ and SH polarizations.

4.1. Description of modes

4.1.1. CaF_2. The lowest-lying mode in figure 3 is the *Rayleigh mode* (S_1) which has $SP_\perp$ polarization (figure 4(*a*)); it extends through the entire SBZ. The diminishing of its contribution to $A_{SP_\perp}$ for increasing wavelength ($\bar{q}\rightarrow 0$) in figure 4(*a*) is due to the increasingly deep penetration of the Rayleigh mode with increasing wavelength, which diminishes the participation of the surface particles in the mode. At the $\overline{K}$ point there occurs a crossing of two branches of the Rayleigh mode. In the lower branches at the crossing the particles in neighbouring layers vibrate in-phase, whereas in the upper branches the particles in neighbouring layers vibrate in opposite phase. These latter branches lose their surface-localized character as soon as they enter the bulk bands on either side of $\overline{K}$. Low-lying $SP_\parallel$ and SH modes, which are often found at the (001) surfaces of alkali halides (cf [10]), are practically absent in the case of CaF_2. At 7.8 THz we find, near $\overline{\Gamma}$, a pair of *Lucas modes* (Lu), of which the lower mode has SH polarization and extends over a large part of the interval $\overline{\Gamma}\,\overline{M}$. The upper mode with SP polarization merges with the bulk bands, close to $\overline{\Gamma}$. A second pair of *Lucas modes* is found in the neighbourhood of $\overline{\Gamma}$ at 8.4 THz. Just above it, at 8.56 THz at $\overline{\Gamma}$, lies a mode with $SP_\perp$ polarization (corresponding to the mode S_2 in the alkali halides); it is also confined to the neighbourhood of $\overline{\Gamma}$. Finally in the band gap at $\overline{K}$ there is a very pronounced SH mode at around 11 THz.

Except for the Rayleigh mode, the modes just described are all *microscopic* surface modes, which means that their amplitudes diminish very rapidly away from the surface, for all wavelengths. The Rayleigh mode is a *macroscopic* surface mode in that its penetration into the crystal increases with the wavelength (see above). The other well-known example of a macroscopic mode pair are the optical *Fuchs–Kliewer modes* (FK), which have SP

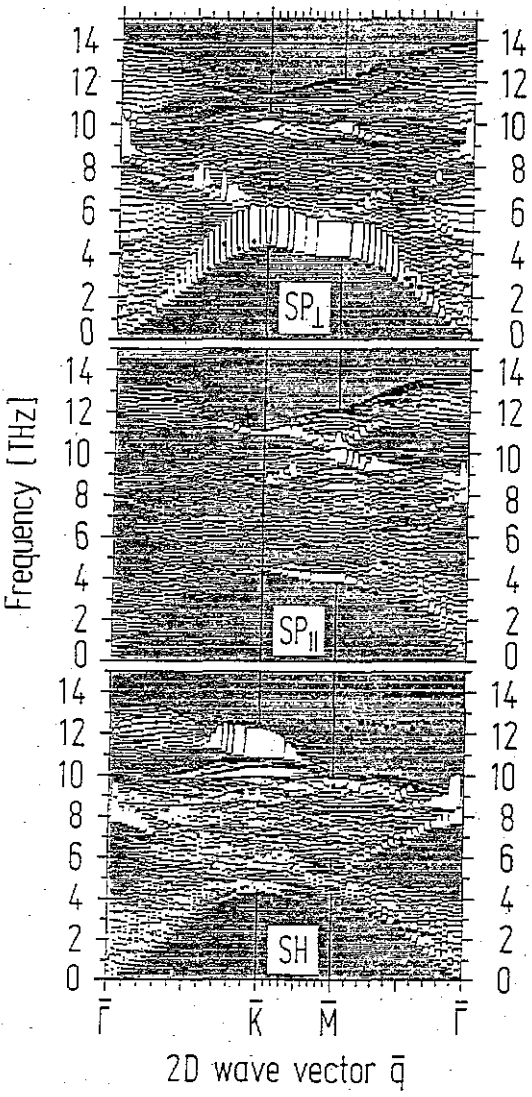

Figure 4. Plots of the normalized surface squared amplitude $A_\alpha(l_3 = 1; \bar{q}\omega)$ of $CaF_2(111)$, corresponding to the dispersion curves of figure 3, for $\alpha = SP_\perp$, $SP_\parallel$ and SH.

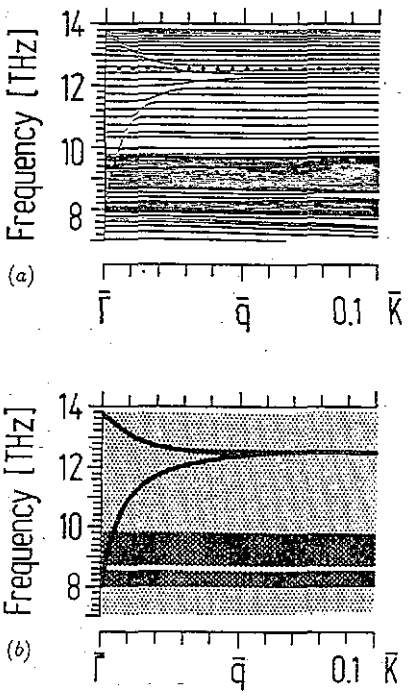

Figure 5. (*a*) Fuchs–Kliewer (FK) modes as loci of hybridizations in the LO and TO bulk bands of a 23-layer slab of CaF_2 with free (111) surfaces, for small 2D wave vectors along $\bar{\Gamma}$ $\bar{K}$. The dotted line indicates the FK frequency for a slab of infinite thickness. (*b*) FK mode frequencies for a continuum dielectric slab of CaF_2 of thickness as in (*a*), as obtained from (6), for small 2D wave vectors along $\bar{\Gamma}$ $\bar{K}$. The bulk frequencies are indicated by the shading.

polarization and appear as loci of hybridizing branches in the longitudinal optical (LO) and transverse optical (TO) bulk bands near $\bar{\Gamma}$ (for a detailed description see Chen *et al* [11]). This situation is shown in figure 5(*a*) in which the dispersion curves for a 23-layer slab are plotted for the $\bar{\Gamma}\bar{K}$ direction for a limited wave vector range near $\bar{\Gamma}$. At $\bar{\Gamma}$ the upper branch

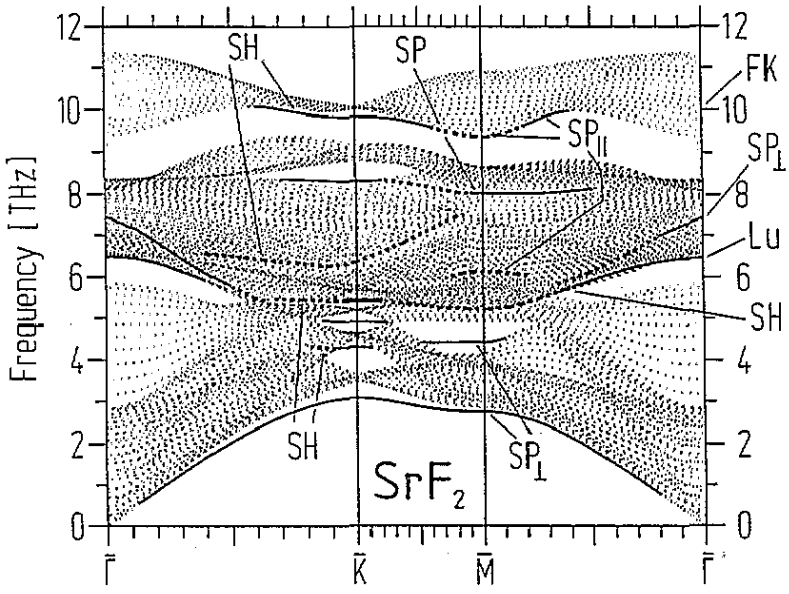

Figure 6. Dispersion curves for a 19-layer slab of SrF_2 with free (111) surfaces. (Same explanations apply as for figure 3).

starts at the top of the upper LO band, and the lower branch at the bottom of the lower TO band. As $\bar{q}$ increases the two branches merge in the upper LO band. As the slab thickness is increased the merging occurs closer and closer to $\bar{\Gamma}$, so that in a macroscopic crystal, the macroscopic FK mode has, at $\bar{\Gamma}$, the frequency of the merged branches. Notice that the calculations give the FK frequency at the same value as the measurements [1].

The original work of Fuchs and Kliewer [12] was concerned with optical modes of a dielectric slab in a continuum dielectric description (long-wavelength limit). For a slab of thickness L of a dielectric material such as CaF_2 and SrF_2, which can be described with a single dispersion oscillator (i.e. one ω_{LO} and one ω_{TO}), the Fuchs–Kliewer frequencies as a function of the 2D wave vector $\bar{q}$ are given by [13, 14]

$$\omega^2_{\substack{\text{upper branch}\\ \text{lower branch}}} = \omega^2_{TO}\,\frac{\varepsilon_0 + 1 \pm (\varepsilon_0 - 1)\exp(-\bar{q}L)}{\varepsilon_\infty + 1 \pm (\varepsilon_\infty - 1)\exp(-\bar{q}L)}\,, \tag{6}$$

where ε_0 and ε_∞ are the static and high frequency dielectric constants. The dependence of the FK mode frequencies on the wave vector $\bar{q}$ and slab thickness L, as given by our microscopic calculations in the long-wavelength limit, are in excellent agreement with equation (6). The results following from (6) for a 23-layer slab are plotted in figure 5(*b*).

As can be seen from figure 4 not all of the measured points of [1] can be identified as surface modes or resonances. In some cases it is a matter of judgement how the measurements should be interpreted.

4.1.2. SrF_2. The dispersion curves for a 19-layer slab and the normalized surface-projected densities of states are displayed in figures 6 and 7, respectively. Since the mass ratio of SrF_2 is twice that of CaF_2 the bulk bands are more separated, creating gaps in which well-defined surface modes can occur (figure 6). As a result, the surface modes extend, in general, over larger parts of the SBZ than in the case of CaF_2; nevertheless many of the comments made

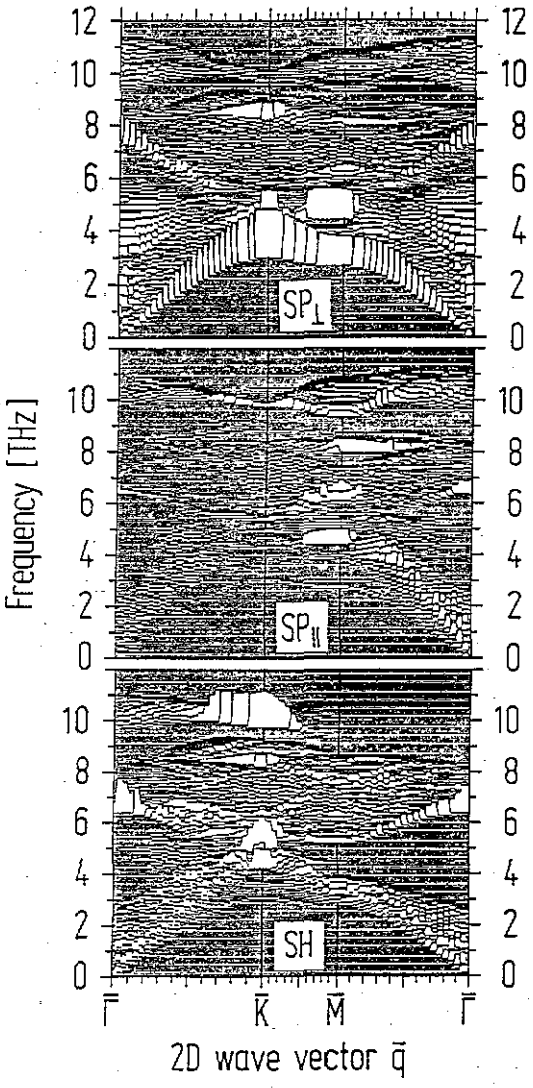

Figure 7. Plots of the normalized surface squared amplitude $A_\alpha(l_3 = 1; \bar{q}\omega)$ of $SrF_2(111)$, corresponding to the dispersion curves of figure 6, for $\alpha = SP_\perp$, $SP_\parallel$ and SH.

for CaF_2 apply here as well. Some distinct differences with CaF_2 are the following. (i) Only one pair of *Lucas modes* at about 6.5 THz is present (corresponding to the lower pair in CaF_2). (ii) There are three additional gaps at $\overline{K}$ and one at $\overline{M}$, all of which contain surface modes as indicated in figure 6. The lowest of these modes at $\overline{K}$ (at 4.64 THz), is predominantly horizontally polarized and the main vibration takes place in the second layer. In the mode at 5.39 THz the topmost F ion vibrates perpendicular to the surface, while the other two particles in the first layer vibrate in the plane with an even larger amplitude. Finally, the mode at 5.45 THz is mainly a vibration of the Sr ion in the second layer.

5. Final comment

We have emphasized on a number of occasions in the past (cf e.g., [10, 6(a)]) that surface relaxation and surface vibrations provide much more demanding and stringent tests for

ionic interaction models than bulk properties do, because of the many cancellations which occur in bulk interactions as the result of bulk symmetry. For instance, because of the strong relaxation of the outer F^- layer in $CaF_2(111)$ and $SrF_2(111)$, the relaxation and surface dynamical results provide a very stringent test for the interaction potentials at short distances. As a result static and dynamic phenomena at the cleavage planes of the fluorites may be better suited for comparative testing of potential models than those at the cleavage planes of the NaCl and CsCl structure crystals.

Acknowledgments

One of us (F W de Wette) acknowledges support by the Robert A Welch Foundation (Grant F-433) and by the donors of the Petroleum Research Fund, administered by the American Chemical Society. A NATO travel grant is gratefully acknowledged.

References

[1] Longueville J L, Thiry P A, Pireaux J J and Caudano R 1990 *Phonons 89* ed S Hunklinger *et al* (Singapore: World Scientific) p 895. In the original figure of this paper the measurements of the FK mode appear as a dispersionless mode throughout the Brillouin zone. However, since no crystal momentum is transferred to this mode, the measured frequency should be plotted at the point $\bar{\Gamma}$ only.

[2] Lakshmi G and Srinivasan R 1978 *Proc. Int. Conf. on Lattice Dynamics (Paris, 1977)* ed M Balkanski (Paris: Flammarion) p 305

[3] Lakshmi G and de Wette F W 1980 *Surf. Sci.* **94** 232

[4] CaF_2: Elcombe M M and Pryor A W 1970 *J. Phys. C: Solid State Phys.* **3** 492

[5] SrF_2: Elcombe M M 1972 *J. Phys. C: Solid State Phys.* **5** 2702

[6] (a) For a review of the general method see e.g.:
Reiger R, Prade J, Schröder U, de Wette F W, Kulkarni A D and Kress W 1989 *Phys. Rev.* B **39** 7938
(b) For details of the present calculation see:
Jockisch A 1991 *Doctoral Dissertation*, Universität Regensburg

[7] Lehner N, Rauh H, Strobel K, Geick R, Heger G, Bouillot J, Renker B, Rousseau M and Stirling W G 1982 *J. Phys. C: Solid State Phys.* **15** 6545

[8] de Wette F W, Kress W and Schröder U 1985 *Phys. Rev.* B **32** 4143

[9] (a) Prade J, Schröder U, Kress W, Kulkarni A D and de Wette F W 1990 *Phonons 89* ed S Hunklinger *et al* (Singapore: World Scientific) p 946
(b) Prade J, Schröder U, Kress W, de Wette F W and Kulkarni A D 1993 *J. Phys.: Condens. Matter* **5** 1

[10] Kress W, de Wette F W, Kulkarni A D and Schröder U 1987 *Phys. Rev.* B **35** 5783

[11] Chen T S, de Wette F W and Alldredge G P 1977 *Phys. Rev.* B **15** 1167

[12] Fuchs R and Kliewer K L 1965 *Phys. Rev.* **140** A2076

[13] Bryskin V V and Firsov Yu A 1970 *Sov. Phys.–Solid State* **11** 1751

[14] Kliewer K L and Fuchs R 1974 *Adv. Chem. Phys.* **27** 335